Role of Local Structure in the Enhanced Dynamics of Deformed Glasses

Entao Yang and Robert A. Riggleman[*]

Department of Chemical and Biomolecular Engineering, University of Pennsylvania, Philadelphia, Pennsylvania 19104, USA

External stress can accelerate molecular mobility of amorphous solids by several orders of magnitude. The changes in mobility are commonly interpreted through the Eyring model, which invokes an empirical activation volume. Here, we analyze constant-stress molecular dynamics simulations and propose a structure-dependent Eyring model, connecting activation volume to a machine-learned field, softness. We show that stress has a heterogeneous effect on the mobility that depends on local structure through softness. The barrier impeding relaxation reduces more for well-packed particles, which explains the narrower distribution of relaxation time observed under stress.

Introduction.—Stress-induced dynamical acceleration at the molecular level, observed in experiments [1–5] and simulations [6–8], is widely believed to be the origin of yielding and plastic motion in glasses [9–13]. In ductile polymers, this leads to tough materials that can dissipate large amounts of energy before failure, enabling applications in protective coatings and membranes. As a result, understanding how external stress affects polymer dynamics is critical to understanding the mechanism of deformation.

The Eyring model is a classic generic model for describing the effect of external stress on dynamical yielding of activated processes, where an applied stress causes a linear reduction in the energy barrier impeding thermally activated motion [14]. This model and many later modifications [9,15,16] based on the idea that stress can induce faster mobility are still widely employed. However, many studies raise concerns about the validity of this model, mainly from two perspectives: (i) The effective free energy barrier is controlled by an empirical parameter, activation volume, which has neither a clear physical meaning nor a connection to a particle-scale property. (ii) The thermal free energy barrier is assumed to be same everywhere, despite the difference in local structure and potential structural changes in preferred packing during deformation. Both of these concerns can be attributed to the key limitation of the Eyring model, where it does not have a clear structural dependence, neither on a microscopic level nor in an average sense.

It has been long suspected that structure plays an important role in glassy dynamics [17–19], though only recently have structural metrics that are truly predictive of glassy dynamics been developed [20]. Liu and co-workers recently developed a machine-learned field, softness, which characterizes particles' local structure and shows a strong correlation with particle-level dynamics [21–23]. Particles with a higher softness represent that they are more likely to rearrange. This new structural measurement has given insights to many aspects of glassy dynamics, from aging [24] to structural initiation of shear band [25,26]. With softness, bulk glassy dynamics can be decomposed as a product of two independent processes: one that depends on structure through softness, and one that is independent of softness [22,27]. These findings together delineate an inherent connection between structure and dynamics in glassy materials, which further emphasizes the potential for embedding structural components into the Eyring model.

In this study, we refer to particles with relatively high (low) softness as soft(hard) particles and thus soft particles are more likely to rearrange compared to hard particles. We first expand the idea of dynamical decomposition in bulk glass [22,27] to systems undergoing creep deformation. We then prove its validity by proposing a structure-dependent Eyring model that applies within the linear and weakly nonlinear creep region, where the strain rate is constant. Our model connects the activation volume to a structural property (softness) quantitatively for the first time, accounts for the structural heterogeneity, and the model isolates the effect of stress from the structural evolution during deformation. We show that the dynamical enhancement is heterogeneous in the system; hard particles are more sensitive to stress than soft particles and their energy barriers impeding relaxation are reduced more at a given stress, which explains the narrower distributions of relaxation time during deformation observed previously in experiments [10,28–31] and simulations [11,20,30]. This is also consistent with the interpretation suggested by previous work, where dynamical acceleration induced by deformation is higher at slow regions [2].

Methods.—Simulation details: We used a coarse-grained bead-spring model to construct the polymer matrix in our simulation system [32]. Each polymer chain consists of 128 Lennard-Jones (LJ) interaction sites, connected with fully flexible harmonic bonds. Systems are equilibrated in the NPT ensemble at $T = 1.0$ and $P = 0$ with a time step of

$0.002\tau_{LJ}^{-1}$, and then quenched to different target temperatures ($T = 0.35$ to 0.42) near our simulated $T_g = 0.46$ with a same cooling rate, $\Gamma = 10^{-4}\tau_{LJ}^{-1}$, followed by an aging process of $10000\tau_{LJ}$. Creep deformations with a series of stresses ($\sigma_c = 0.1$ to 0.5) are then performed at different temperatures ($T = 0.35$ to 0.42). All the units are in LJ reduced units and simulations are performed using the LAMMPS package [33]. More technical details can be found in the Supplemental Material [34].

Structural measurement—Softness: Softness is a machine-learned field that shows strong correlation with particle-level dynamics [21–23]. Training softness begins by first identifying an equal number of soft particles which are about to rearrange and hard particles that go a long time without rearranging and characterizing their local environment using a group of N_{st} (usually tens to hundreds) structure functions [21,44]. The values of these structure functions form a feature vector for every particle, and each particle corresponds to a point in a high dimensional real space, $\mathbb{R}^{N_{st}}$. By applying a support vector machine (SVM) we can find a hyperplane that best separate the soft particles and the hard particles in $\mathbb{R}^{N_{st}}$. The signed distance between the point and the hyperplane is defined as softness of that particle, which is positive for rearranging side and negative for non-rearranging side. Previous work has shown that particles' rearranging probability increases approximately exponentially with their softness [21–23].

In this study, we use a hyperplane trained previously in a quiescent neat polymer system at $T = 0.50$, where the only difference is polymer chain length. More technical details can be found in the Supplemental Material [34] and our recent work [26]. Our tests suggest softness calculated with this hyperplane follows a normal distribution with a standard deviation $\sigma = 1.0$ and more than 90% of rearranging particles in our system have a positive softness (see Fig. S1 [34]). For the following analysis, unless specified, we focus on the softness ranges from -3.5 to 1.5, covering 98% of particles.

Dynamical measurement—Particles rearranging probability, P_R: Instead of the segmental relaxation time, τ_α, we use particles rearranging probability at a given softness, $P_R(S)$, as the measurement for monomer mobility (see more details in the Supplemental Material [34]). It has been shown that τ_α can be predicted from knowledge of $P_R(S)$ and the softness distribution, where $\tau_\alpha \propto \{1/[P_R(S)]\}$ [22,24]. Materials below their glass transition undergo a process known as physical aging, whereby the material slowly evolves towards equilibrium with an increasing density and reduced mobility. It has been shown that deformation can alter aging dynamics and even reverse its effects (rejuvenation) [29,45,46]. Recent work has shown that the slow glassy dynamics during aging is a structural process (average softness decreases) and the $P_R - S$ relation remains unchanged for different aging times [24]. Thus, an essential advantage of using $P_R(S)$

to measure mobility is that we will be able to separate the effects of stress on the mobility from changes in the structure that arise due to physical aging or rejuvenation.

Results and discussion.—Recent works have shown that the glassy dynamics in the quiescent bulk glassy system [22] and polymer thin films [27] at a given temperature can be decomposed as a product of two independent processes as

$$P_R(S) = \exp\left(\Sigma - \frac{\Delta E}{T}\right) = \exp\left[\left(\Sigma_0 - \frac{e_0}{T}\right)\right],$$

$$\exp\left[-\left(\Sigma_1 - \frac{e_1}{T}\right)S\right] = P_I(T) \cdot P_D(T, S). \quad (1)$$

Here, $P_I(T)$ is structural independent and $P_D(T, S)$ depends on structure through softness, and the four parameters Σ_i and e_i are independent of temperature and softness. We take the same protocol described in the literature [22,27] and start from the quiescent system at a series of T below T_g ($T/T_g = 0.76$–0.91). As shown in Figs. 1(a) and 1(b), we observed a similar trend as a bulk glass system [22], where particles rearranging probability, P_R, exhibits an Arrhenius behavior at each softness, and all the left-extended fitting curves [using Eq. (1)] share a common intersection point. The shared intersection point indicates that Σ and ΔE depend linearly on the softness and the polymer dynamics can be decomposed into two independent parts as shown above in Eq. (1). The corresponding temperature of this intersection point has been demonstrated to scale with the onset temperature of glassy dynamics [22].

We next test whether the dynamical decomposition procedure continues to apply for systems undergoing creep. We performed a series of constant uniaxial, tensile stress MD simulations with stress values ranging from 0.1 to 0.5 while maintaining constant pressure in the transverse directions. The strain-time curves and corresponding softness evolution at the highest temperature ($T = 0.42$) can be found in Figs. 1(e) and 1(f) (see lower T in Fig. S2 [34]). Since our goal is understanding how stress affects the energy barriers of rearranging for a given structure (softness), we primarily focus on the low stress regime where the Eyring model for stress activation has been shown to be most effective [30]. More specifically, we use data collected from $t \in [0, 2000]$ for $\sigma_c \in [0, 0.40]$. While for $\sigma_c = 0.45$, we only use the time period of $t \in [0, 1000]$, before the samples begin to yield. Both the strain and softness changes are larger at $\sigma_c = 0.50$, and we observe larger deviations from the Arrhenius relation at each softness. Thus, we take $\sigma_c = 0.45$ as the upper limit for the decomposition in this work. The system average softness remains unchanged or increases steadily after the initial elastic response within this regime [see Fig. 1(f)]. Our results indicate dynamical decomposition still applies in polymer glasses under external stress, and we observe that the predicted onset temperature (intersection point) shifts to lower values under
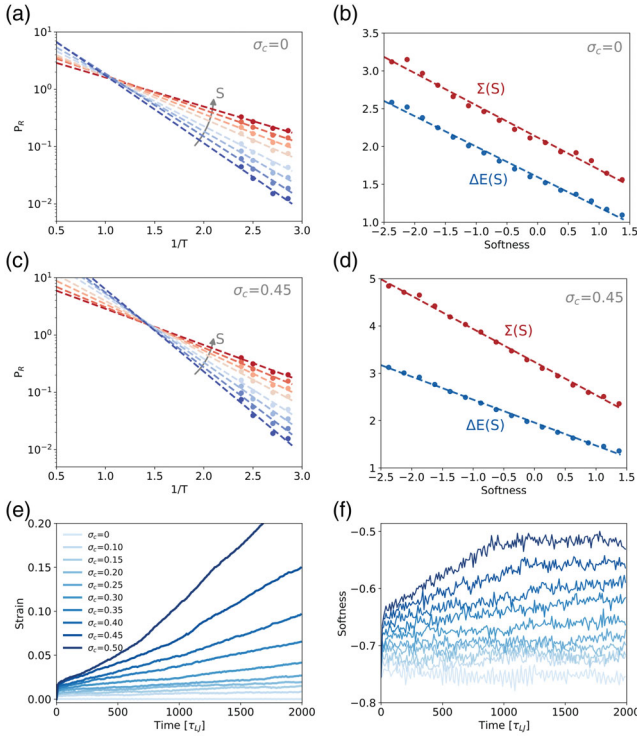
FIG. 1. (a) Polymer monomer rearranging probability at a given softness, $P_R(S)$, versus $1/T$ at different softness values in the quiescent system ($\sigma_c = 0$). The color gradient represents the gradient in softness, ranging from dark blue at lowest S (-2.75) to dark red at highest S (1.25). Dashed lines are fits to an Arrhenius expression, $P_R \propto \exp[-E_A(S)/T]$. (b) Σ (red) and ΔE (blue) versus softness, where $P_R(S) = \exp(\Sigma - \Delta E/T)$. (c) $P_R(S)$ versus $1/T$ in polymers under creep where $\sigma_c = 0.45$. (d) Σ and ΔE in polymers under creep where $\sigma_c = 0.45$. (e) Strain-time curves of polymers under creep at $T = 0.42$. (f) Evolution of average softness in polymers under creep at $T = 0.42$. The color gradient represents the gradient in stress, ranging from light for quiescent system ($\sigma_c = 0$) to dark at the highest stress ($\sigma_c = 0.50$).

deformation, which is consistent with the general notion that mobility can be enhanced by stress [see Figs. 1(c), 1(d), and Fig. S3 [34]].

The Eyring model [14] is widely employed to describe the dynamical acceleration due to external stress in amorphous solids [9,10,30,47,48]. The segmental relaxation time at a certain applied stress, σ_c, can be predicted as $\tau_\alpha \propto \{[\sigma_c]/\sinh[(\sigma_c \cdot V^*)/2k_BT]\}$, where V^* is an empirical activation volume and k_BT is the thermal energy. Physically, V^* controls how strong the mobility depends on the applied stress. Considering $P_R \propto 1/\tau_\alpha$, we expect the changes in P_R due to stress based on the Eyring model to be

$$P_R \propto \frac{\exp(\frac{\sigma_c \cdot V^*}{2k_BT}) - \exp(-\frac{\sigma_c \cdot V^*}{2k_BT})}{2\sigma_c}, \qquad (2)$$

To measure the stress-induced dynamical enhancement, here we introduce a new term, $P_{R,\text{Eyring}} \equiv \{[P_R(S)]/[P_{R,u}(S)]\}$, which is the ratio of P_R during creep relative

to the undeformed system for a given softness. Inserting $P_{R,\text{Eyring}}$ into Eq. (2) and bringing σ_c to the left-hand side, we have for the stress-induced acceleration

$$\sigma_c \cdot P_{R,\text{Eyring}} = A \cdot \left[\exp\left(\frac{\sigma_c \cdot V^*}{2k_BT}\right) - \exp\left(-\frac{\sigma_c \cdot V^*}{2k_BT}\right)\right], \qquad (3)$$

where A is a prefactor. In Fig. 2(a), we plot $\sigma_c \cdot P_{R,\text{Eyring}}$ versus stress for different values of softness at $T = 0.42$, and the measured dynamical enhancement can be nicely described by Eq. (3) for stresses $\sigma_c \leq 0.45$. We choose this temperature because the statistics are usually better at high temperature, since there are more rearrangements, especially for the hard particles, and other temperatures exhibit qualitatively similar behavior (see Fig. S4 [34]). Results in Fig. 2(a) suggest that change of $P_{R,\text{Eyring}}$ agrees well with the Eyring model, which provides a route to look closely at the dynamical expressions of Eq. (1) for glassy polymers under creep. To do so, we first need to address how do the parameters A and V^* depend on softness.

In Figs. 2(b) and 2(c), we plot A and V^* versus softness, finding that A grows exponentially with S while V^* decreases linearly. As a result, we can write $A = \exp(\alpha_1 \cdot S - \alpha_0)$ and $V^* = \beta_0 - \beta_1 \cdot S$, where α_i and β_i are independent of softness. We choose an exponential rather than a linear dependence for the prefactor A because (i) it is unphysical for A to have a negative value and (ii) an exponential relation better matches the other terms in the dynamical decomposition model. Note that unlike the parameters (Σ_i and e_i) we have in the original ($\sigma_c = 0$)
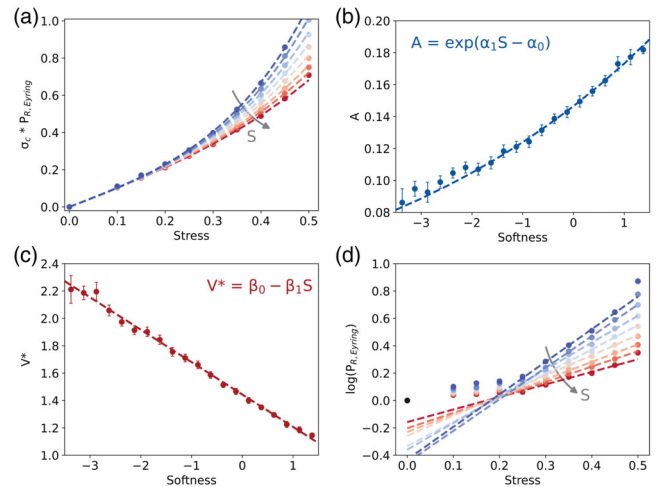

FIG. 2. (a) $\sigma_c \cdot P_{R,\text{Eyring}}$ versus stress at different softness. The dash curves are fitted using Eq. (3) for $\sigma_c \leq 0.45$ (with parameters A and V^*). (b) The prefactor A and (c) activation volume V^* versus softness. Error bars represent the standard deviation of uncertainty. (d) $\log P_{R,\text{Eyring}}$ versus stress at different softness [fit for $0.3 \leq \sigma_c \leq 0.45$ using Eq. (5)]. The softness color gradient represents the same gradient presented in Figs. 1(a) and 1(c).

model, we observe that α_i and β_i depend on T (see Fig. S4 [34]), which is expected because the magnitude of dynamical enhancement for a given stress can vary strongly with T. If we put the expressions for A and V^* into Eq. (3) and combine with the above expression $P_R(S) = P_{R,u}(S) \cdot P_{R,\text{Eyring}}(S)$, we can arrive at a complete expression for polymer dynamics under creep,

$$P_R(S) = \frac{\exp(\alpha_1 \cdot S - \alpha_0)}{\sigma_c} \cdot \left[\exp \frac{\sigma_c \cdot (\beta_0 - \beta_1 \cdot S)}{T} \right.$$
$$\left. - \exp \left(-\frac{\sigma_c \cdot (\beta_0 - \beta_1 \cdot S)}{T} \right) \right]$$
$$\cdot \exp \left[\left(\Sigma_0 - \frac{e_0}{T} \right) \right] \cdot \exp \left[-\left(\Sigma_1 - \frac{e_1}{T} \right) S \right]. \quad (4)$$

We refer to this model as the structure-dependent Eyring model. Note that we have not taken any approximations beyond the functional forms of each term, so we expect this relationship to hold if we restrict ourselves within the low stress regime, where both the Eyring model and the dynamical decomposition remain valid.

Because of the existence of the hyperbolic sine term, it seems that we cannot as easily separate (decompose) the dynamics for systems under creep deformation into distinct structure dependent and independent terms. However, our simulations show that the negative exponential term decays rapidly with stress. In other words, when stress is not too small ($\sigma_c \geq 0.25$), Eq. (4) can be written approximately as

$$P_R(S) \approx \frac{1}{\sigma} \cdot \exp \left(\Sigma_0 - \alpha_0 + \frac{\beta_0 \cdot \sigma_c - e_0}{T} \right)$$
$$\cdot \exp \left[-\left(\Sigma_1 - \alpha_1 + \frac{\beta_1 \cdot \sigma_c - e_1}{T} \right) \cdot S \right]. \quad (5)$$

From Eq. (5) we can see that P_R can be approximated as a product of two exponential terms when external stress is large enough, where one depends on softness and the other does not. This makes P_R have a similar form as Eq. (1), explaining why dynamical decomposition works in this situation.

In the limit of small applied stress, $\{[\sigma_c \cdot (\beta_0 - \beta_1 \cdot S)]/T\}$ is close to 0, and a Taylor expansion for the sinh term yields $\{[2\sigma_c \cdot (\beta_0 - \beta_1 \cdot S)]/T\}$, which is not an exponential term and appears to preclude dynamical decomposition. However, when stress is small, the dynamical change is also insignificant and $P_{R,\text{Eyring}}$ is nearly 1, allowing us to assume the effects of stress can be decomposed. Thus, the dynamical decomposition is valid in both cases, consistent with the results presented in the last section.

The Eyring activation volume physically measures the stress sensitivity of overall energy barrier for rearrangements, and V^* is regarded as a volume because $([\sigma_c \cdot V^*]/[2k_BT])$ need to be dimensionless. It has

generally been considered as an empirical fitting parameter that has not yet been connected to a microscopic structure [9,10,16]. Traditionally, the activation volume V^* also does not change with stress for a given material at constant temperature. However, our results indicate that V^* is not constant but heterogeneous in glassy polymers, and furthermore it decreases linearly with softness, a measurement of particles local structure. This finding puts the activation volume on similar footing as the activation energy in quiescent glass-forming materials, which is known to be heterogeneous and intimately connected to the local structure [21–23]. For the harder particles, which is less likely to rearrange even under deformation, the larger activation volume corresponds to a larger decrease in the energy barrier for rearrangements. Integrating $V^* = \beta_0 - \beta_1 \cdot S$ over the softness distribution at different stress yields an overall V^* similar to traditional values, $V^* \approx 1.6$, which agrees with the interpretation that V^* is the cooperative movement of two to three segments [10]. Our results also show that this overall V^* depends weakly on stress, since external stress can slightly increase the mean softness.

Based on our derivation above, there are two different regimes for polymer dynamical enhancement under linear creep. When the stress is sufficiently small (i.e., the two stress-involved exponential terms are in the same order of magnitude), the dynamical acceleration is relatively small, leading to a weak dependence on particles local environment. When the stress becomes larger (but not so large as to induce yielding and an increasing strain rate), polymer dynamics can be expressed as a product of two independent processes for a given stress.

In Fig. 2(d), we plot $\log P_{R,\text{Eyring}}$ versus stress at $T = 0.42$ and find a turning point that indicates this crossover in behavior at approximately $\sigma_c = 0.25$. Below this stress, the dynamical enhancement is relatively small, although there is still a weak dependence on the structure. After this point, the enhancement grows exponentially with stress, and the growth is larger for the hard particles. This threshold value and unsmoothed dependences of the mobility on stress has been observed in experiments [1]. The fitting curves of different softness share a common intersection point, which is expected from the linear relation between activation volume and softness. In other words, for polymer glass under creep, the dynamical enhancement directly depends on the local structure, and the mobility acceleration is larger for the hard particles compared with soft particles. Considering softness is intimately related to the barrier for particle rearrangements in glassy systems [22], our results suggest this barrier decreases more under stress for harder particles.

While this heterogeneous acceleration offsets the heterogeneous structure in the polymer glass, the structural heterogeneity remains unchanged during creep, as evidenced by the constant variation of softness distribution (see Fig. S5 [34]). This ultimately leads to a narrower

distribution of mobility for polymer under external stress, which can be confirmed from the dynamical heterogeneity measured through the KWW stretching exponent (see Fig. S6 [34]).

Conclusion.—In summary, we have demonstrated that in glassy polymer systems the dynamics can be decomposed into two independent processes, and this decomposition can be further expanded to systems under creep, at least within the low stress regime. By introducing a dynamical enhancement ratio, $P_{R,\mathrm{Eyring}}$, we show particles that are less likely to rearrange in the quiescent state have their energy barrier for rearrangement reduced more than particles that are prone to rearranging, as indicated by the larger activation volume for the hard particles. To the best of our knowledge, this is the first time that the activation volume has been correlated with a particle-scale property. We also reveal that there is a turning point for the dynamical enhancement for polymer glass under external load, as predicted by the structural-dependent Eyring model. When the stress is small, the acceleration is small and the dependence on structure is weak. When it is sufficiently large enough and make the negative exponential term in the Eyring model negligible, the dynamical enhancement grows exponentially with stress and shows a strong dependence on softness. As shown previously, regions with lower softness have a higher local density [27]. Thus, the mobility of denser-packed particles accelerates more under external stress. This heterogeneous dynamical enhancement reduces the dynamical heterogeneity caused by the structure, which remains unchanged under stress, and leads to the narrower mobility distribution observed in polymer glass under active deformation.

---

*rrig@seas.upenn.edu

[1] M. D. Ediger, H. N. Lee, K. Paeng, and S. F. Swallen, Dye reorientation as a probe of stress-induced mobility in polymer glasses, J. Chem. Phys. **128**, 034709 (2008).

[2] H.-N. Lee, K. Paeng, S. F. Swallen, M. D. Ediger, R. A. Stamm, G. A. Medvedev, and J. M. Caruthers, Molecular mobility of poly(methyl methacrylate) glass during uniaxial tensile creep deformation, J. Polym. Sci., Part B: Polym. Phys. **47**, 1713 (2009).

[3] J. Ricci, T. Bennin, E. Xing, and M. D. Ediger, Linear stress relaxation and probe reorientation: Comparison of the segmental dynamics of two glassy polymers during physical aging, Macromolecules **52**, 8177 (2019).

[4] D. Bonn, H. Tanaka, P. Coussot, and J. Meunier, Ageing, shear rejuvenation and avalanches in soft glassy materials, J. Phys. Condens. Matter **16**, S4987 (2004).

[5] P. Agarwal and L. A. Archer, Strain-accelerated dynamics of soft colloidal glasses, Phys. Rev. E **83**, 041402 (2011).

[6] R. A. Riggleman, H.-N. Lee, M. D. Ediger, and J. J. de Pablo, Free Volume and Finite-Size Effects in a Polymer Glass under Stress, Phys. Rev. Lett. **99**, 215501 (2007).

[7] R. A. Riggleman, K. S. Schweizer, and J. J. De Pablo, Nonlinear creep in a polymer glass, Macromolecules **41**, 4969 (2008).

[8] J. Rottler, Relaxation times in deformed polymer glasses: A comparison between molecular simulations and two theories, J. Chem. Phys. **145**, 064505 (2016).

[9] K. Chen and K. S. Schweizer, Stress-enhanced mobility and dynamic yielding in polymer glasses, Europhys. Lett. **79**, 2 (2007).

[10] H.-N. Lee, K. Paeng, S. F. Swallen, and M. D. Ediger, Direct measurement of molecular mobility in actively deformed polymer glasses, Science **323**, 231 (2009).

[11] R. A. Riggleman, H. N. Lee, M. D. Ediger, and J. J. De Pablo, Heterogeneous dynamics during deformation of a polymer glass, Soft Matter **6**, 287 (2010).

[12] K. Chen and K. S. Schweizer, Theory of yielding, strain softening, and steady plastic flow in polymer glasses under constant strain rate deformation, Macromolecules **44**, 3988 (2011).

[13] S. M. Fielding, R. G. Larson, and M. E. Cates, Simple Model for the Deformation-Induced Relaxation of Glassy Polymers, Phys. Rev. Lett. **108**, 048301 (2012).

[14] H. Eyring, Examples of absolute reaction rates, J. Chem. Phys. **4**, 283 (1936).

[15] K. Chen and K. S. Schweizer, Theory of aging, rejuvenation, and the nonequilibrium steady state in deformed polymer glasses, Phys. Rev. E **82**, 041804 (2010).

[16] D. R. Long, L. Conca, and P. Sotta, Dynamics in glassy polymers: The eyring model revisited, Phys. Rev. Mater. **2**, 105601 (2018).

[17] M. L. Manning, J. S. Langer, and J. M. Carlson, Strain localization in a shear transformation zone model for amorphous solids, Phys. Rev. E **76**, 056106 (2007).

[18] C. P. Royall, S. R. Williams, T. Ohtsuka, and H. Tanaka, Direct observation of a local structural mechanism for dynamic arrest, Nat. Mater. **7**, 556 (2008).

[19] M. L. Manning and A. J. Liu, Vibrational Modes Identify Soft Spots in a Sheared Disordered Packing, Phys. Rev. Lett. **107**, 108302 (2011).

[20] D. Richard, M. Ozawa, S. Patinet, E. Stanifer, B. Shang, S. A. Ridout, B. Xu, G. Zhang, P. K. Morse, J.-L. Barrat, L. Berthier, M. L. Falk, P. Guan, A. J. Liu, K. Martens, S. Sastry, D. Vandembroucq, E. Lerner, and M. L. Manning, Predicting plasticity in disordered solids from structural indicators, Phys. Rev. Mater. **4**, 113609 (2020).

[21] E. D. Cubuk, S. S. Schoenholz, J. M. Rieser, B. D. Malone, J. Rottler, D. J. Durian, E. Kaxiras, and A. J. Liu, Identifying Structural Flow Defects in Disordered Solids using Machine-Learning Methods, Phys. Rev. Lett. **114**, 108001 (2015).

[22] S. S. Schoenholz, E. D. Cubuk, D. M. Sussman, E. Kaxiras, and A. J. Liu, A structural approach to relaxation in glassy liquids, Nat. Phys. **12**, 469 (2016).

[23] E. D. Cubuk *et al.*, Structure-property relationships from universal signatures of plasticity in disordered solids, Science **358,** 1033 (2017).

[24] S. S. Schoenholz, E. D. Cubuk, E. Kaxiras, and A. J. Liu, Relationship between local structure and relaxation in out-of-equilibrium glassy systems, Proc. Natl. Acad. Sci. U.S.A. **114,** 263 (2017).

[25] R. J. S. Ivancic and R. A. Riggleman, Identifying structural signatures of shear banding in model polymer nanopillars, Soft Matter **15,** 4548 (2019).

[26] E. Yang, R. J. S. Ivancic, E. Y. Lin, and R. A. Riggleman, Effect of polymernanoparticle interaction on strain localization in polymer nanopillars, Soft Matter **16,** 8639 (2020).

[27] D. M. Sussman, S. S. Schoenholz, E. D. Cubuk, and A. J. Liu, Disconnecting structure and dynamics in glassy thin films, Proc. Natl. Acad. Sci. U.S.A. **114,** 10601 (2017).

[28] R. Besseling, E. R. Weeks, A. B. Schofield, and W. C. K. Poon, Three-Dimensional Imaging of Colloidal Glasses under Steady Shear, Phys. Rev. Lett. **99,** 028301 (2007).

[29] H. N. Lee and M. D. Ediger, Interaction between physical aging, deformation, and segmental mobility in poly (methyl methacrylate) glasses, J. Chem. Phys. **133,** 014901 (2010).

[30] H.-N. Lee, R. A. Riggleman, J. J. de Pablo, and M. D. Ediger, Deformation-induced mobility in polymer glasses during multistep creep experiments and simulations, Macromolecules **42,** 4328 (2009).

[31] C. Eisenmann, C. Kim, J. Mattsson, and D. A. Weitz, Shear Melting of a Colloidal Glass, Phys. Rev. Lett. **104,** 035502 (2010).

[32] K. Kremer and G. S. Grest, Dynamics of entangled linear polymer melts: A molecular-dynamics simulation, J. Chem. Phys. **92,** 5057 (1990).

[33] S. Plimpton, Fast parallel algorithms for short-range molecular dynamics, J. Comput. Phys. **117,** 1 (1995).

[34] See Supplemental Material at http://link.aps.org/supplemental/10.1103/PhysRevLett.128.097801 for softness distribution, results for other temperature and stresses, discussion on dynamical enhancement and heterogeneity, and details of softness training, P_R measurements, and MD simulations, which includes Refs. [10,21–24,26,27,29,32,33,35–43].

[35] R. A. Riggleman, G. N. Toepperwein, G. J. Papakonstantopoulos, and J. J. De Pablo, Dynamics of a glassy polymer nanocomposite during active deformation, Macromolecules **42,** 3632 (2009).

[36] R. Candelier, A. Widmer-Cooper, J. K. Kummerfeld, O. Dauchot, G. Biroli, P. Harrowell, and D. R. Reichman, Spatiotemporal Hierarchy of Relaxation Events, Dynamical Heterogeneities, and Structural Reorganization in a Supercooled Liquid, Phys. Rev. Lett. **105,** 135702 (2010).

[37] A. Smessaert and J. Rottler, Distribution of local relaxation events in an aging three-dimensional glass: Spatiotemporal correlation and dynamical heterogeneity, Phys. Rev. E **88,** 022314 (2013).

[38] E. D. Cubuk, S. S. Schoenholz, E. Kaxiras, and A. J. Liu, Structural properties of defects in glassy liquids, J. Phys. Chem. B **120,** 6139 (2016).

[39] M. L. Falk and J. S. Langer, Dynamics of viscoplastic deformation in amorphous solids, Phys. Rev. E **57,** 7192 (1998).

[40] W. Li, J. M. Rieser, A. J. Liu, D. J. Durian, and J. Li, Deformation-driven diffusion and plastic flow in amorphous granular pillars, Phys. Rev. E **91,** 062212 (2015).

[41] N. C. Karayiannis, V. G. Mavrantzas, and D. N. Theodorou, A Novel Monte Carlo Scheme for the Rapid Equilibration of Atomistic Model Polymer Systems of Precisely Defined Molecular Architecture, Phys. Rev. Lett. **88,** 105503 (2002).

[42] B. J. Banaszak and J. J. De Pablo, A new double-rebridging technique for linear polyethylene, J. Chem. Phys. **119,** 2456 (2003).

[43] R. Auhl, R. Everaers, G. S. Grest, K. Kremer, and S. J. Plimpton, Equilibration of long chain polymer melts in computer simulations, J. Chem. Phys. **119,** 12718 (2003).

[44] J. Behler and M. Parrinello, Generalized Neural-Network Representation of High-Dimensional Potential-Energy Surfaces, Phys. Rev. Lett. **98,** 146401 (2007).

[45] J. J. Martinez-Vega, H. Trumel, and J. L. Gacougnolle, Plastic deformation and physical ageing in PMMA, Polymer **43,** 4979 (2002).

[46] H. N. Lee and M. D. Ediger, Mechanical rejuvenation in poly(methyl methacrylate) glasses? Molecular mobility after deformation, Macromolecules **43,** 5863 (2010).

[47] C. A. Angell, K. L. Ngai, G. B. McKenna, P. F. McMillan, and S. W. Martin, Relaxation in glassforming liquids and amorphous solids, J. Appl. Phys. **88,** 3113 (2000).

[48] R. J. Hunter, *Foundations of Colloid Science* (Oxford University Press, New York, 2001).